Projection of surface ozone over East Asia in 2020

Masayuki Takigawa[1]†, Masanori Niwano[1],
Hajime Akimoto[1], Masaaki Takahashi[1,2], and Kazuhiko Kobayashi[3]
[1] *Frontier Research Center for Global Change, Kanagawa, Japan*
[2] *Center for Climate System Research, University of Tokyo, Ibaraki, Japan*
[3] *Graduate School of Agricultural and Life Science, The University of Tokyo, Tokyo*

Abstract

To evaluate the impact of emission change in East Asia on the surface ozone concentration, one–year calculations with emission inventory for 2000 and 2020 were conducted by using a one–way nested global–regional chemical transport model (CTM) system. This model consists of the global and regional CTMs. The global CTM is based on the CHASER (chemical atmospheric general circulation model for study of atmospheric environment and radiative forcing) model, while the regional part is based on the WRF (weather research and forecasting) / Chem model. Anthropogenic emissions in East Asia was taken from REAS (Regional Emission inventory in ASia). Comparison of the modeled surface ozone with ground–based observation at Mt. Tai showed that the model generally reproduced diurnal variations of ozone in the North China Plain. By comparing the horizontal distribution of surface ozone concentration, ozone decrease by 1–3 ppbv were seen in the North China Plain where the increase of ozone precursors is most remarkable, and increase by 3–10 ppbv were also seen in the outflow region of the North China Plain, such as Sichuan, Korea, and Japan. The comparison of diurnal variations of surface ozone in the North China Plain in 2000 and 2020PFC showed that ozone maximum increased by 10% in 2020PFC from 2000, because of enhanced ozone production in the daytime.

keyword: surface ozone, chemical transport model, future projection, East Asia, diurnal variation

1. Introduction

Tropospheric ozone has been recognized as a harmful pollutant for decades, and East Asia is a region in which anthropogenic emissions are considered to be rapidly increasing and are predicted to increase further (Akimoto 2003; Ohara et al. 2007). The concentration of surface ozone over Japan is strongly affected by the regional transport from East Asian emissions especially in summer (Pochanart et al. 2006), and such an outflux from East Asia can affect to the ozone concentration on a global scale (Wild et al. 2004).

Thus, it is quite important to predict the ozone concentration over East Asia in near future for the prediction of air quality over downstream region such as Japan. Some studies have applied regional CTMs for the future prediction of tropospheric ozone. Wang et al. (2005) developed a source–specific high–resolution emission inventory for eastern China for 2000 and 2020, and showed that surface O_3 concentration will be decrease around urban areas in eastern China due to increased NO_x emissions and VOC–limited O_3 chemistry. Yamaji et al. (2008) also executed model calculation for the future prediction in East Asia for 2000 and 2020, and showed that O_3 concentration averaged within PBL will be increase by 7–50% in summer over the North China Plain (NCP). Ozone production rate is strongly affected by the quantity of NO_x and volatile organic compounds (VOC), and the positive and negative tendency of O_3 in the future prediction will depend on the ratio of NO_x and VOC emission increase and chemical reactions considered in the model.

To estimate the change of ozone concentration over East Asia in present and future, we have applied a one-way nested global-regional CTM (chemical transport model) with the present (2000) and future (2020) emission inventories.

2. Numerical model and emission inventories

An global–regional CTM system has been developed based on the WRF/Chem and the CHASER (Takigawa et al. 2007; Niwano et al. 2007). As the lateral boundary of chemical species in the regional CTM part is taken from the global CTM part with the time interval of 6 hours, this model is able to treat long–range transport, in situ chemistry, and local–scale transport within the polluted area simultaneously. Both of the regional and global CTMs are "online" model, *i.e.,* transport of chemical species is done using the same vertical and horizontal coordinates with the meteorological part of the model, and the same physics parametrization with no interpolation in time.

The global CTM part is based on the CHASER model, which is based on CCSR/NIES/FRCGC atmospheric general circulation model (AGCM) version 5.7b (Sudo et al. 2002b,a; Takigawa et al. 2005). Spectral coefficients are triangularly truncated at wavenumber 42 (T42), equivalent to a horizontal grid spacing of about 2.8°. The model has 32 vertical layers that are spaced at approximately 1–km intervals in the free troposphere and lower stratosphere.

The regional CTM part is based on WRF/Chem (Grell et al. 2005). Although WRF has several choices for dynamical cores, in the present study we use the mass coordinate version of the model, called Advanced Research WRF (ARW) version 2.1.2. Gas–phase chemistry in the model is following to RADM2 (Stockwell et al. 1990). Anthropogenic surface emissions over the East Asia are taken from REAS with $0.5° \times 0.5°$ resolution (Ohara et al. 2007), and surface emissions over Russia are taken from EDGAR (Emission Database for Global Atmospheric Re-

†Corresponding author: Masayuki Takigawa, Frontier Research Center for Global Change, Japan Agency for Marine–Earth Science and Technology, 3173–25 Showa–machi, Kanazawa–ku, Yokohama, Kanagawa 235–0001, Japan. E-mail: takigawa@jamstec.go.jp

search) 2000 with 1°×1° resolution (Olivier et al. 1996). The biomass burning emissions especially form crop recidue buring are quite important for the source of ozone precursors in China (Yang et al. 2008), and biomass burning emissions are also taken from the EDGAR2000. Diurnal variations of anthropogenic surface emissions are parametrized in emissions from REAS and EDGAR2000 following averaged variations of JCAP (Japan Clean Air Program) (*K. Murano, personal communication*). Biogenic emissions are based on Guenther et al. (1993). Figure 1 shows the model domain for the regional CTM part, and the horizontal resolution is 40–km (199×149 grids). The regional CTM have 31 vertical layers up to 100 hPa, and there are 11–12 layers at the height of 0–2 km from the surface.

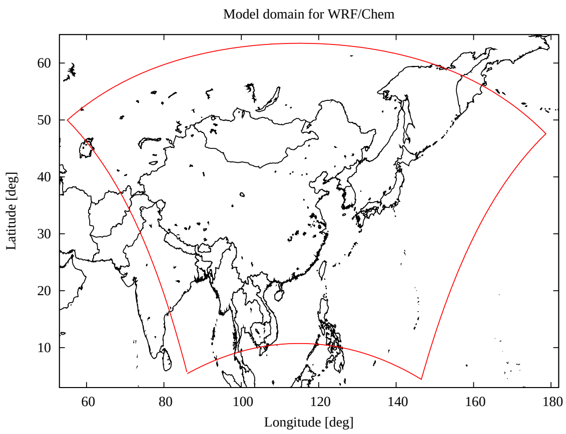

Figure 1 Red line denotes model domain for the regional CTM part.

The system is driven by meteorological data from the National Centers for Environmental Prediction (NCEP) The output of the global CTM part is monotonically interpolated from the Gaussian latitude and longitude grid to the Lambert Conformal conic projection for the use in the regional CTM part. The lateral boundary is updated every 6 hours and linearly interpolated for each time step. In this study, we did not take feedback from the regional CTM part to the global CTM part; that is, the one–way nesting calculation has been done between the global and regional CTMs.

To evaluate the impact of anthropogenic emissions over East Asia on O_3 concentration in East Asia, two model calculations have been conducted with REAS emissions for 2000 and 2020 (Ohara et al. 2007). There are three scenarios for China (REF: Reference Case, PSC: Policy Succeed Case, and PFC: Policy Failed Case) in REAS emission inventories for future prediction, and PFC case is applied for the present study. PFC scenario is the most pessimistic scenario with high emission increases caused by continuation of current energy supply structure, increased energy consumption, and slow developments of new energy and emission control technologies. The PSC scenario resemble the A2 scenario of IPCC. Total fuel consumption is expected to increase by 77% in 2020PFC from 2000 in China, and NO_xemission over China in 2000 and 2020PFC is estimated to be 11.2 Tg/yr and 25.4 Tg/yr, respectively (cf. Ohara et al. 2007). Each experiment was integrated for one year from January to December after a spinup calculation for one month, and calculated values such as ozone were recorded every one hour to evaluate the change of diurnal variation of surface ozone.

3. Results

Before comparing O_3 concentration among calculations for 2000 and 2020, the surface ozone mixing ratio calculated with the inventory for 2000 was compared to that observed at ground–based observational station in China, although O_3 concentration calculated by using this model has been already evaluated with ground–based observations at 251 stations in Japan (cf. Takigawa et al. 2007). Figure 2 shows monthly–mean diurnal variations of ozone concentration at Mt. Tai (36.25°N, 117.10°E, 1536m) observed in July, 2006 (*P. Pochanart, personal communication*) with model–calculated ozone at the nearest grid (red colors). Mt. Tai locates within the North China Plain, and ozone concentration at Mt. Tai sometimes exceeds 120 ppbv in the observation. In general, the model reproduced diurnal variation of ozone. The minimum value of O_3 concentration is 70.4 ppbv in the observation and 70.8 ppbv in the model at 8:00 CST (Chinese Standard Time), and the maximum value in observation and model is 93.7 ppbv and 88.8 ppbv at 16:00 CST, respectively. The model slightly underestimate the amplitude of ozone increase in the daytime. Increase of ozone is 2.25 ppbv/hour in the model, and 2.99 ppbv/hour in the observation. This discrepancy may be caused by the lack of temporal variation in biomass burning emissions from waste crop burning in the present study.

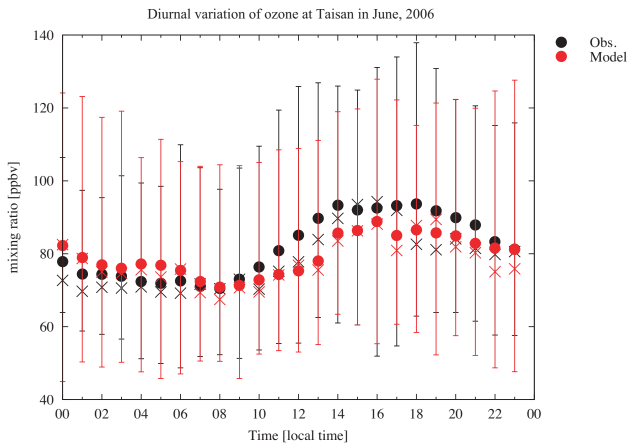

Figure 2 Observed (black) and calculated (red) monthly–mean diurnal variations of ozone concentration at Mt. Tai (36.25°N, 117.10°E, 1536m). Unit is ppbv. Circles, crosses, and vertical bars denotes average, median, and 1–σ, respectively

Figure 3a shows the horizontal distribution of monthly–mean, 24 hour–averaged surface ozone concentration in July 2000. High ozone concentration can be seen around the edge of Tibetan plateau. High ozone concentration over Tibetan plateau can be also seen the results of other models (cf. Li et al. 2007). Downstream region of mountainous region such as Tibetan plateau might be affected by the effect of stratosphere–troposphere exchange (STE), because the wind field is influenced by the mountain waves (Ding and Wang 2006). High ozone concentration can be also seen in the northern part of India, and ozone concentration exceeds 60 ppbv even in monthly-mean and 24–hour average. Anthropogenic emissions of ozone precursors are quite large, and photochemistry is also active in that region. Figure 3b shows the horizontal distribution of ozone increase at surface in 2020PFC from 2000. Ozone concentration increase by 5–10 ppbv in Sichuan, but decreases by 1–3 ppbv in the North China Plain. NO_x emission in the North China Plain increase by 49% in REAS inventories in 2020PFC from 2000 (cf. Yamaji et al. 2008), and NO_x increase also enhances ozone destruction in the nighttime. Ozone concentration in Korea and Japan increases by 3–8 ppbv. Ozone concentration in Tibetan plateau is not strongly affected by the change of emissions over East Asia. This result implies that most of ozone in Tibetan plateau is not photochemically produced from precursors emitted in East Asia, and long–range transport or STE might affect ozone concentration in that region. Ozone increase by 5–10 ppbv can be seen in the Sea of China, and it is mainly due to the increase of emissions along international ship track.

(a)

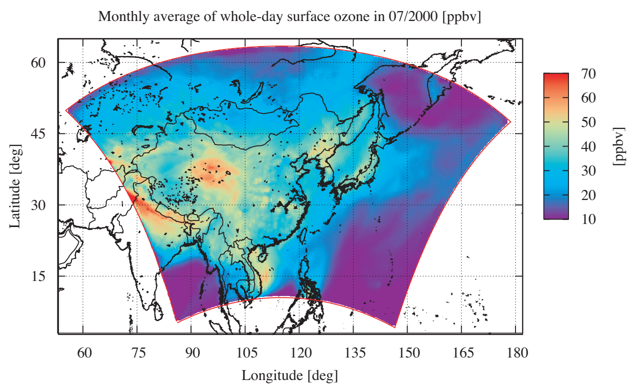

(b)

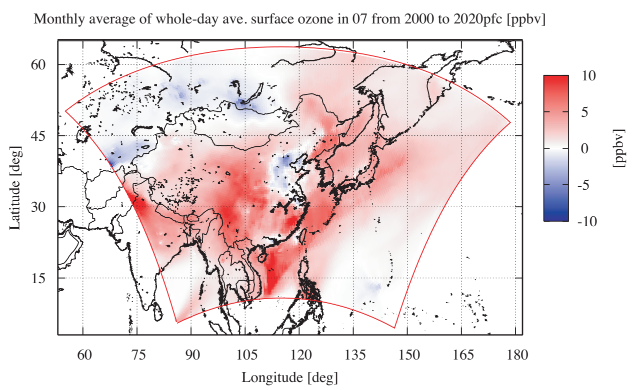

Figure 3 Latitude–longitude cross section of monthly–mean 24hour–averaged ozone concentration at surface in July 2000 (a), and difference of surface ozone from 2000 at the policy failed case in 2020 (b). Units are ppbv.

To reveal the impact of emission change on ozone variation in the North China Plain, diurnal variation of ozone in 2020PFC is compared to that in 2000. Figure 4 shows the monthly–mean diurnal variation of ozone concentration averaged in the North China Plain ($114°$E–$119°$E, $37°$N–$41°$N) in July. The maximum value of averaged ozone concentration is almost same in 2000 and 2020PFC, but the destruction of ozone in the nighttime is larger in 2020PFC. The maximum value of 90–percentile of ozone concentration is 90.3 ppbv at 16 CST in 2020PFC, and 82.1 ppbv at 16 CST in 2000. In contrast, the maximum value of 10–percentile decreases by 3 ppbv in 2020PFC (27.7 ppbv) from 2000 (31.23 ppbv). These results shows that the day–to-day variation of daytime ozone increases by 40% in 2020PFC from 2000. That is, ozone production increases in sunny days in 2020PFC because of increased VOC and NO_x emission, and ozone destruction also increases because of increased NO_x emission. Minimum values in the morning are almost same in 2000 and 2020PFC, because ozone concentration in the morning is almost zero by nighttime titration in both cases.

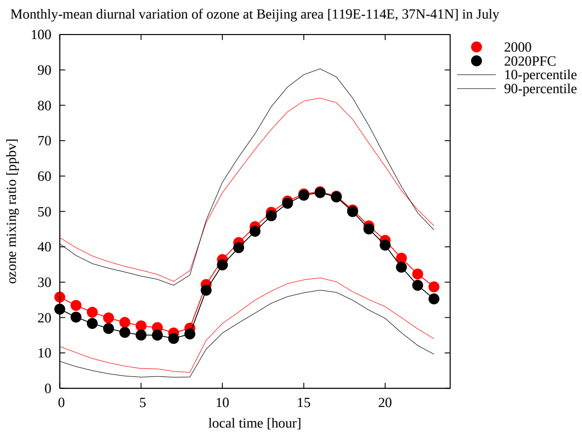

Figure 4 Monthly–mean diurnal variation of surface ozone concentration in the North China Plain ($114°$E–$119°$E, $37°$N–$41°$N) in July. Unit is ppbv. Red colors are for 2000, and black colors are for 2020PFC. Circles denotes average, and thin lines denote 10–percentile and 90–percentile values.

4. Summary and discussion

A one–way nested global–regional CTM was developed to simultaneously treat long–range transport and local transport and chemistry over East Asia. The model system covers East Asia with the horizontal resolution of 40–km. Vertical intervals in the planetary boundary layer is 50–200 m, and it also includes lower stratosphere in the regional and global CTM. Comparison of the modeled surface ozone with ground–based observation at Mt. Tai showed that the model generally reproduced diurnal variations of ozone in the North China Plain. The model could not reproduce day–to–day variation of ozone levels especially in the nighttime, suggesting that improvements of the treatment of biomass burning emission is needed for more precise estimation of ozone concentration. To evaluate the impact of emission change in East Asia on the surface ozone concentration, one–year calculations with emission inventory for 2000 and 2020 were conducted. By comparing the horizontal distribution of surface ozone concentration, ozone decrease by 1–3 ppbv were seen in the North China Plain where the increase of ozone precursors is most remarkable, and increase by 3–10 ppbv were also seen in the outflow region of the North China Plain, such as Sichuan, Korea, and Japan. The result suggests that nighttime ozone destruction by NO_x prevent from increasing ozone concentration even though daytime ozone production is enhanced by increased VOC and NO_x emissions in the source region. The comparison of diurnal variations of surface ozone in the North China Plain in 2000 and 2020PFC suggested that ozone maximum increased by 10% in 2020PFC from 2000, because of enhanced ozone production in the daytime. Minimum value of ozone decreased by 10%, because of enhanced ozone destruction in the nighttime.

WRF/Chem, which is applied to the regional part of this model, is an online model and enables to consider the effect of small scale perturbation to the transport of chemical species. Niwano et al. (2007) showed the model well reproduced the ozone layer above the nocturnal residual layer observed in the suburban area in Japan. This polluted air remains even in daytime at the height of 1–2 km, because of longer lifetime of short–lived species compared to the surface. The existence of such ozone layer might affect to the outflux of ozone into the Pacific, and the estimation of vertical integrated ozone flux should be evaluated.

Acknowledgments

The authors would like to thank Dr. G. Grell, Prof. K. Sudo, and all others responsible for the development of the WRF/Chem and CHASER models.

References

Akimoto, H., 2003: Global air quality and pollution. *Science*, **302**, 1716–1719.

Ding, A., T. Wang, 2006: Influence of stratosphere–to–troposphere exchange on the seasonal cycle of surface ozone at Mount Waliguan in western China. *Geophys. Res. Lett.*, **33**, doi:doi:10.1029/2005GL024760.

Grell, G. A., S. E. Peckham, R. Schmitz, et al., 2005: Fully coupled "online" chemistry within the WRF model. *Atmos. Environ.*, **39**, 6957–6975.

Guenther, A., P. R. Zimmerman, P. Harley, et al., 1993: Isoprene and monoterepene emission rate variability: Model evaluations and sensitivity analyses. *J. Geophys. Res.*, **98D**, 12,609–12,617.

Li, J., Z. Wang, H. Akimoto, et al., 2007: Modeling study of ozone seasonal cycle in lower troposphere over east Asia. *J. Geophys. Res.*, **112**, doi:doi:10.1029/2006JD008209.

Niwano, M., M. Takahashi, M. Takahashi, et al., 2007: Evaluation of vertical ozone profiles simulated by WRF/Chem using Lidar–observed data. *SOLA*, **3**, 133–136, doi:10.2151/sola.2007-034.

Ohara, T., H. Akimoto, J. Kurokawa, et al., 2007: Asian emission inventory for anthropogenic emission sources during the period 1980–2020. *Atmos. Chem. Phys.*, **7**, 4419–4444.

Olivier, J. G. J., A. F. Bouwman, C. W. M. Van der Maas, et al., 1996: Description of EDGAR Version 2.0. A set of global emission inventories of greenhouse gases and ozone-depleting substances for all anthropogenic and most natural sources on a per country basis and on $1° \times 1°$ grid. *RIVM/TNO rep.*, RIVM, Bilthoven, number nr. 711060 002, 1006.

Pochanart, P., J. Hirokawa, Y. Kajii, et al., 2006: Influence of regional–scale anthropogenic activity in northeast Asia on seasonal variations of surface ozone and carbon monoxide observed at Oki, Japan. *J. Geophys. Res.*, **104**, 3621–3631, doi:10.1029/1998JD10071.

Stockwell, W., P. Middleton, J. Chang, et al., 1990: The second–generation regional acid deposition model chemical mechanism for regional air quality modeling. *J. Geophys. Res.*, **95**, 16343–16367.

Sudo, K., M. Takahashi, H. Akimoto, 2002a: CHASER: A global chemical model of the troposphere 2. Model results and evaluation. *J. Geophys. Res.*, **107**, doi:10.1029/2001JD001114.

Sudo, K., M. Takahashi, J. Kurokawa, et al., 2002b: CHASER: A global chemical model of the troposphere 1. Model description. *J. Geophys. Res.*, **107**, doi:10.1029/2001JD001113.

Takigawa, M., M. Niwano, H. Akimoto, et al., 2007: Development of an one–way nested global–regional air quality forecasting model. *SOLA*, **3**, 81–84, doi:10.2151/sola.2007-021.

Takigawa, M., K. Sudo, H. Akimoto, et al., 2005: Estimation of the contribution of intercontinental transport during PEACE campaign by using a global model. *J. Geophys. Res.*, **110**, doi:10.1029/2005JD006226.

Wang, X., D. L. Mauzerall, Y. Hu, et al., 2005: A high–resolution emission inventory for eastern China in 2000 and three scenarios for 2020. *Atmos. Environ.*, **39**, 5917–5933, doi:doi:10.1016/j.atmosenv.2005.06.051.

Wild, O., M. J. Prather, H. Akimoto, et al., 2004: Chemical transport model ozone siulations for spring 2001 over the western Pacific: Regional ozone production and its global impacts. *J. Geophys. Res.*, **109**, doi:doi:10.1029/2003JD004041.

Yamaji, K., T. Ohara, I. Uno, et al., 2008: Future prediction of surface ozone over East Asia using Models–3 Community Multiscale Air Quality Model System (CMAQ) and Regional Emission Inventory in ASia (REAS). *J. Geophys. Res.*, **in press**.

Yang, S., H. He, S. Lu, et al., 2008: Global air quality and pollution. *Atmos. Environ.*, **42**, 1961–1969, doi:doi:10.1016/j.atmosenv.2007.12.007.